SYNOPTIC: Some Characteristics of Exhaust Plume Rarefaction, E. P. Muntz, B. B. Hamel, and B. L. Maguire, General Electric Company, Valley Forge, Pa.; *AIAA Journal*, Vol. 8, No. 9, pp. 1652–1658.

Jets; Rarefield Flows

Theme

Discusses rarefaction phenomena in highly underexpanded exhaust plumes.

Content

Analyzes exhaust plume rarefaction from continuum flow to scattering regime. A rarefaction parameter is found that will correlate certain of the rarefaction phenomena from shock broadening to the penetration of background gas into the core of the plume. The parameter is

$$\xi = D(P_S P_{B\infty})^{1/2}/T$$

where D = sonic orifice diameter, cm; P_s = stagnation chamber pressure, dynes/cm^2; $P_{B\infty}$ = background pressure, dynes/cm^2; and T = temperature, °K.

Experimental results for molecular beam facilities are shown to be consistent with the scaling. Experimental measurement of the plume shock broadening are shown to be correlated by ξ.

Background gas is predicted to penetrate to a distance r_P from the exit orifice of the underexpanded flow:

$$r_p = \epsilon \bar{V}_\infty \pi \sigma_{Bj}{}^2 n^* r^{*2}/\bar{C}_B{}^1$$

where $\bar{V}_\infty$ = relative velocity, σ_{Bj} = background-jet collision diameter, n^* = sonic number density, r^* = sonic radius, and $\bar{C}_B{}^1 = f(\bar{C}_B)$, background mean molecular speed.

Some Characteristics of Exhaust Plume Rarefaction

E. P. Muntz,* B. B. Hamel,† and B. L. Maguire‡
General Electric Company, Valley Forge, Pa.

In this paper the rarefaction of a free jet expanding into a region of finite background pressure is considered. It is found that the rarefaction process can be described by a simple rarefaction parameter $D(P_s P_{B\infty})^{1/2}/T$. Here D is the sonic orifice diameter, P_s is the reservoir pressure, $P_{B\infty}$ is the background pressure and T is the background and reservoir temperatures which are considered to be the same. A simple scattering formulation of the complex physical problem is proposed. Comparison of the scattering prediction and previous molecular beam flux measurements by Fenn and Anderson are presented. A consistent physical description of a plume's approach to the limit of expansion into a perfect vacuum is discussed.

Nomenclature

$\bar{C}$ = mean molecular speed
D = sonic orifice diameter, cm
k = Boltzmann's constant
n = number density, molecules/cc
P = pressure, dynes/cm^2
$\mathfrak{R}$ = density ratio across shock
r = distance along jet streamline
T = temperature, °K
V = velocity
$\bar{V}$ = relative velocity; $\bar{V}_\infty = V_\infty + \bar{C}_B{}^1$
X_M = distance from sonic orifice to the Riemann wave
δ = shock thickness
γ = ratio of specific heats
λ = mean free path
μ = viscosity
ν = collision frequency
σ = collision diameter
ξ = rarefaction parameter, $\xi = D(P_s P_{B\infty})^{1/2}/T$

Superscripts

* = reference or sonic condition

Subscripts

B = background molecule
jI = ideal jet condition
j = jet molecule
s = stagnation region condition
∞ = freestream

Presented as Paper 69-657 at the AIAA Fluid and Plasma Dynamics Conference, San Francisco, Calif., June 16–18, 1969; submitted March 10, 1969; revision received March 9, 1970. The authors would like to thank A. L. Cooper for useful discussions during the course of this investigation. E. Strybuc was a significant contributor to the experimental work. Support for the work was received from the Air Force Office of Scientific Research, Mechanics Division; the Office of Naval Research, Project Squid; and the General Electric Company.

* Consultant, Environmental Sciences Laboratory Section, at present Associate Professor, University of Southern California, Los Angeles, Calif. Associate Fellow AIAA.

† Associate Professor, Drexel Institute of Technology, Philadelphia, Penn.

‡ Consultant, Environmental Sciences Laboratory.

1. Introduction

THE continuum to rarefied transitional behavior of exhaust plumes is considered. Phenomena that are discussed are associated with the transition from a low altitude

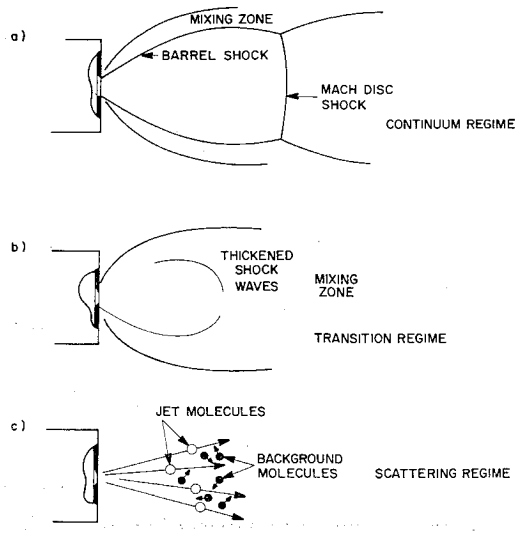

Fig. 1 Regimes describing plume rarefaction.

continuum plume with Rankine-Hugoniot shock waves to one at a very high altitude with no shock waves. Details of the transition are presented. Also, a description is given of some of the features of a plume's approach to the limit of expansion into a perfect vacuum.

The general exhaust plume problem can be very complex indeed when chemical relaxation, reactions, and multispecies effects are included. Since the purpose here is to investigate the continuum-rarefied transition, the discussion is simplified to a single component gas which flows through a highly underexpanded sonic orifice. Moreover, it is assumed that the source Reynolds number is large enough so that the plume gases reach limiting velocity before significant rarefaction occurs. Although this represents a simplification of the general plume problem, it permits an isolation of the rarefaction effects.

In studying a plume as it is raised from low altitude to very high altitude it is instructive to consider it to be in one of three flow regimes. These regimes are illustrated schematically in Fig. 1.

At low altitudes the plume is in the continuum regime; the shock waves are described by a Rankine-Hugoniot relation. In this regime the shock waves mark the inner limit of the effect of background gas. As the altitude is increased the shock waves become thick, reducing the size of the plume's undisturbed core. This regime, which is typified by very thick shock waves that gradually lose their Rankine-Hugoniot character, will be called the transition regime.

As the altitude is increased still further, the shock waves become so thick that they lose their identity as gas dynamic features. They are more easily thought of as extensive zones in which background gas diffuses into the plume, eventually scattering the plume molecules. Plumes in which such scattering is dominant will be considered to be in a scattering regime. As the background density continues to decrease, the scattering zone thickens progressively and the perfect vacuum limit of the scattering regime is approached. The plume rarefaction process has been clearly presented in the motion picture *Rarefied Gas Dynamics*.[1]

In the sections that follow these regimes are considered in more detail. A quantitive picture of the continuum-rarefied plume transition is constructed.

2. Continuum Freejet

Although the discussion will center on rarefaction effects in high altitude plumes it is valuable to be acquainted with the characteristics of the low altitude, or continuum limit of the plume since it is departures from this picture that are to be discussed.

In Fig. 2 the structure of a continuum plume is clearly exhibited. The technique that was used to obtain these pictures was the electron beam flow visualization technique.[2] This technique and the related electron beam fluorescence technique[3,4] for gas specie density measurements are appealed to frequently in the following investigation of rarefied plumes. A short digression will be made at this point to describe these experimental techniques.

In the electron beam flow visualization technique an unattenuated beam of high-energy electrons is oscillated in a plane, which in these experiments contains the plume axis. The electron beam excites emission from the various gas species in the flow at different characteristic wavelengths. The intensity of the emission varies directly as the species density and the beam current density. Thus, in the fan of electrons created by the oscillating beam the density at any point will be related to the emission intensity at that point. The emission intensity at one point will be related to the emission intensity at any other point by the density difference and beam current density difference. The beam current density is known and increases towards the apex of the fan. In order to record the information, an image intensifier camera is used. The system will give the density at any point in the fan by measuring the blackening on a calibrated film. The sheet or fan of emission is only about 1 mm thick so that the technique does not integrate along a line-of-sight but provides density field visualization for a plane cut through the flow.

By employing different filters in the optical path, different gas species can be examined. Also, in certain cases specie concentration are obtained by holding the beam stationary and measuring intensity at appropriate wavelengths with photomultiplier tubes.[3,4] This technique was used for some of the measurements reported later.

The dark areas in Fig. 2a indicate high helium density and the lighter areas indicate lower helium density. In this case the plume and background were helium, except that a very small amount of nitrogen was added to the background. Only the nitrogen was observed in Fig. 2b by the use of a suitable filter, the dark areas on the film represent high background concentration. In both Figs. 2a and 2b, two photographs were taken in order to cover a greater area of the flow. It is evident that there are multiple cells associated with this high pressure ratio plume.

The discussion of the properties of a continuum plume can now be resumed. Most of the flowfield in this limit can be calculated using the method of characteristics which results in an internal core surrounded by the barrel shock waves and the Mach disc shock. A core of inviscid expansion exists

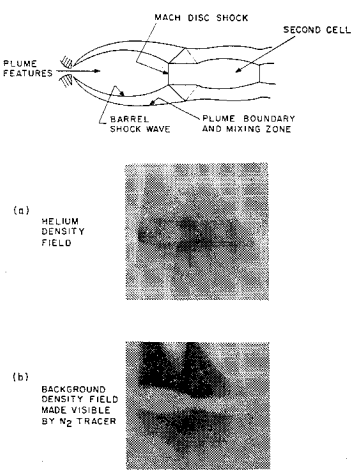

Fig. 2 Continuum regime plume density field as illuminated by the electron beam flow visualization technique.

around the plume centerline. It has been found that the Mach number may be described by a simple expression that can be modeled by a source flow approximation.[5] As the gas expands it encounters background gas; the background gas is excluded from the inviscid core by a shock system which includes an oblique shock barrel, a free mixing layer and a normal shock Mach disc. Ashkenas and Sherman[5] give for the position of the Mach disc,

$$X_M/D = 0.67(P_s/P_{B_\infty})^{1/2} \tag{1}$$

where P_s is the source pressure and P_{B_∞} the background pressure. In the inviscid region Ashkenas and Sherman also give a very simple expression for the plume density,

$$n(r,\theta) = n(r,0)\cos^2\frac{\pi\theta}{2.73}; \quad \gamma = 1.667 \tag{2}$$

$$n(r,0) = 0.161 n_s(D/r)^2 \tag{3}$$

where r is distance from exit orifice and θ is measured from the plume axis. In the low altitude region the plume consists of a series of similar cells, where only the first is known to exhibit a structure described by the above relations although subsequent cells appear quite similar as can be seen from Fig. 2. The downstream cells seem to become progressively more rarefied so that rarefaction effects are observed to move toward the sonic orifice through successive cells. Because very little is known about the properties of these cells discussions of the transition and scattering in Sec. 3 will only be concerned with the first one.

3. Transition and Scattering Regimes

In this section, the thickening of the continuum shock wave and its eventual dissolution into a diffuse scattering region is considered on a quantitative basis. The interaction of background gas and a freejet can be resolved into the collisional interaction of two distinct classes of particles: hyperthermal freejet molecules and thermalized background molecules.

First, the transition regime is considered where the mixing zone is thin and a clearly defined hydrodynamic shock wave occurs. In this limit, a single length scale suffices for the description of the interaction zone thickness. As the zone thickens and the plume passes into the scattering regime it is necessary to consider the dynamics of each stream. To do this a scattering theory is formulated which takes into account the spatially nonuniform collisional frequencies associated with each class of molecule.

As a consequence of these formulations a rarefaction parameter is found that is common to both the transition and scattering regimes.

The rarefaction process can be seen in Fig. 3 which shows plume density fields obtained using the electron beam visualization technique. These photographs show a progressive increase in rarefaction from 1 to 4. A constant pressure ratio was maintained during the rarefaction of the plume; therefore, the continuum-limit shock wave positions are the same for all of the photographs.

The most obvious effect of increased rarefaction is the destruction of a clearly recognizable normal shock or Riemann wave at the base of the plume. It appears that the barrel shock waves collapse, or rather grow and gobble-up the normal shock. After this the boundary quickly forms a continuous region of density adjustment surrounding the inner core of the plume. The undisturbed inner core region persists deep into the rarefaction process until the shock envelope disappears entirely and the plume enters the scattering regime. Another feature of the rarefaction is that in all cases (with a constant pressure ratio) the general position of the shock envelope remains about the same until it simply vanishes. A similar result was found in Pitot pressure surveys made by Ashkenas and Sherman.[5]

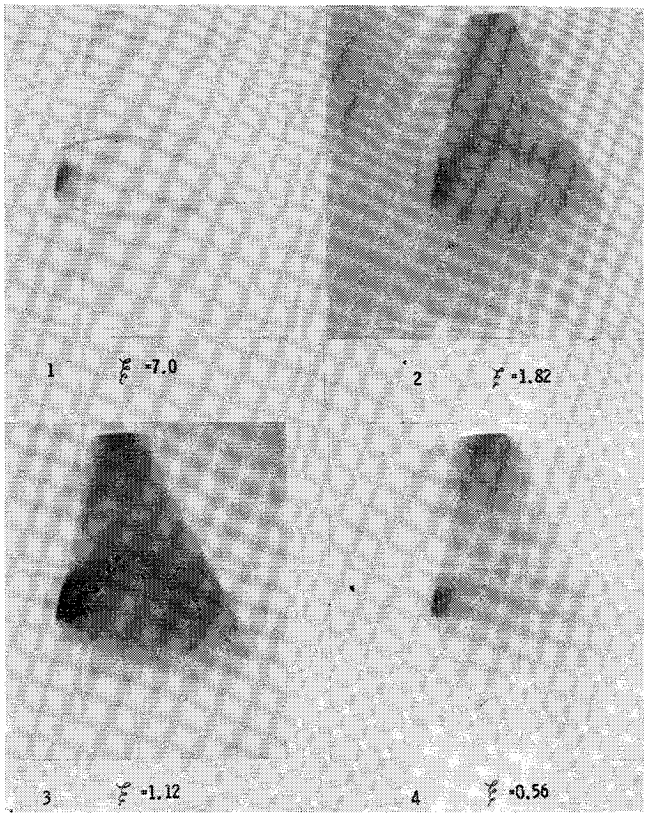

Fig. 3 Helium plume rarefaction $P_s/P_{B_\infty} = 1 \times 10^3$, $D = 0.2$ cm.

A. Transition Regime

The broadening of a normal shock wave in the plume field can be thought of as either the broadening of the initial normal shock or Riemann wave at the base of the plume, or the broadening of the shock envelope after the oblique shock's destruction of the Riemann wave. Due to the complication of the problem, the following analysis is at best approximate, but it will be seen to provide some useful information about rarefaction phenomena in the transition regime. Broadening is only considered along the jet centerline.

The shock wave on the jet centerline broadens in a hypersonic flow. To express the shock thickness a reference length L^* is introduced after Talbot and Sherman,[6] based on a reference viscosity μ^* where the reference viscosity is obtained from the temperature $T^* = 2T_s/(\gamma + 1)$. In the plume the freestream velocity closely approximates the escape velocity of the gas (V_∞). A maximum slope shock thickness can be expressed in terms of the reference length as $\delta_{SHI} = KL^*$. If an inverse power repulsion is assumed for the molecular interaction such that $\mu = \mu_0 T^s$, the reference length can be put in terms of the stagnation conditions and the freestream density. The maximum slope shock thickness becomes

$$\delta_{SHI} = \chi/n_j = \left\{\frac{5K2^{(s-1/2)}(\gamma-1)^{1/2}}{16\sigma_s^2\pi^{1/2}(\gamma+1)^s\gamma^{1/2}}\right\}\Big/ n_{j1} \tag{4}$$

where σ_s is the stagnation region collision diameter. Also n_{j1} is the undisturbed number density immediately upstream of the shock wave.

In terms of L^* the maximum slope shock thickness asymptotes to some constant (K) for hypersonic flows. It will be assumed for the plume flows that this limit has been reached.

To describe the shock thickening relative to the plume the thickness of the shock is compared to a characteristic plume dimension. This is particularly attractive in this case because the geometric form of the continuum plume is quite similar for a wide variety of conditions. In addition, the shock

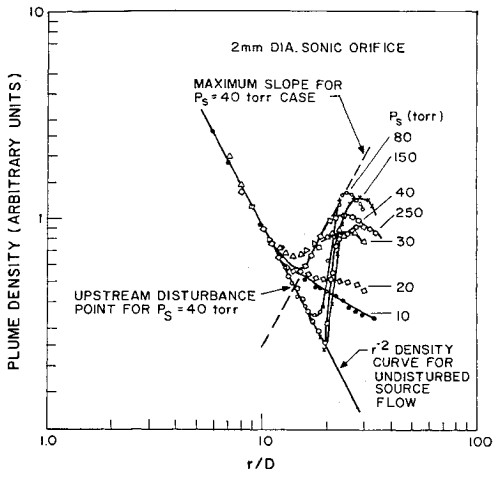

Fig. 4 Centerline helium density for various rarefield plumes from 0.2 cm diam sonic orifice at $P_s/P_{B_\infty} = 1 \times 10^3$.

envelope does not change position significantly during rarefaction at a constant pressure ratio. A characteristic plume dimension was taken to be the distance X_M from the sonic orifice to the Riemann wave. The dimension X_M is related to the pressure ratio by Eq. (1).

When the radial nature of the jet flow is considered the maximum slope shock thickness divided by X_M becomes

$$\delta_{SHA}/X_M = (\delta_{SHI}/X_M)[1/(1 + \delta_{SHI}/X_M)] \quad (5)$$

where

$$\delta_{SHI}/X_M = (\chi \mathcal{R} k/0.67)[T_1/D(P_sP_{B_\infty})^{1/2}] \quad (6)$$

is the shock thickness in a parallel flow divided by X_M. $\mathcal{R}$ is the density ratio across the shockwave; k is the Boltzmann constant and

$$\chi = [5K2^{(s-1/2)}(\gamma - 1)^{1/2}]/[16\sigma_s^2\pi^{1/2}(\gamma + 1)^s\gamma^{1/2}] \quad (7)$$

The shock thickening relative to the plume size is a function solely of the rarefaction variable $D(P_sP_{B_\infty})^{1/2}/T = \xi$. The larger ξ becomes, the closer continuum conditions are approached. Different gases of course produce an effect which is evidenced by changes in the parameters χ and $\mathcal{R}$. In all cases it has been assumed that the pseudo source used in the radial approximation[5] is located at the sonic orifice. For ratios of specific heats other than 5/3 this is not quite as good as approximation as is available.[5]

As an initial attempt to test the applicability of the plume shock broadening predictions, a few experiments have been completed. These results are presented in Fig. 4 where the centerline densities for several helium plumes are shown.

Note that in these measurements the collapse of the oblique shock waves to the plume axis appears as a large increase in the density jump. To compare experiments and theory, it was decided that rather than trying to estimate shock thickness directly, it was preferable to locate the point at which the measured density is 10% greater than the calculated jet density. This point is an indication of the spreading of the shock into the plume. A comparison has been made between the distance of this disturbance point from the sonic orifice and the calculated value for $[1 - (\delta_{SHA}/X_M)]$. The comparison is shown in Fig. 5a for helium, 5b for nitrogen. For the comparison the following values are used to calculate δ_{SHA}/X_M: helium, $K = 6.5$, $\mathcal{R} = 4$, and $s = 0.647$; nitrogen, $K = 6.5$, $\mathcal{R} = 6$, and $s = 0.768$; all values appropriate to shock waves in a hypersonic flow which has expanded from room temperature.

For helium, prediction and experiments match quite reasonably to a δ_{SHA}/X_M of about 0.5 after which they separate. It is for about this range of conditions that the axial density profiles (Fig. 4) indicate that the concept of a normal shock wave with roughly the right density jump (factor of four) applies. For the more rarefied plumes ($\delta_{SHI}/X_M > 1.0$), the density jump drops significantly below a factor of four. Therefore, the very lower end of the transition regime might be defined empirically on this basis at $\delta_{SHA}/X_M = 0.5$ or $\delta_{SHI}/X_M \approx 1.0$ for helium. The corresponding rarefaction parameter can be found as $D(P_sP_{B_\infty})^{1/2}/T \approx 2.5k/\sigma_s^2$.

For nitrogen, prediction, and experiments match quite reasonably to a δ_{SHA}/X_M of about 0.6 or $\delta_{SHI}/X_M = 1.5$. The corresponding rarefaction parameter is $(D(P_sP_{B_\infty})^{1/2}/T) \approx 2.2k/\sigma_s^2$.

Thus, for a plume from a sonic orifice to be in a flow regime that can be described in a continuum sense, $\xi \geq 2k/\sigma_s^2$. Broader applicability of this scaling remains to be studied.

Perhaps the main characteristic of Eq. (5) is that the description of a shock thickness only involves a single length scale; the mean free path of a background molecule in the jet. When the interaction region becomes very diffuse a second length becomes important; the mean free path of a jet molecule in the background gas. In the discussion of the scattering regime that follows, the behavior of both of these lengths is described.

B. Scattering Regime

As illustrated by the series of photographs in Fig. 3, there exists a rarefied regime for plumes from underexpanded sonic orifices where any evidence of continuum gas dynamic features has disappeared. This contention is supported by the density measurements in Fig. 4. For the $P_s = 10$ torr helium case, the shock envelope has completely vanished and the gas density smoothly passes to the background density through scattering processes. The existence of such a regime was first suggested by Fenn and Anderson[7] to explain their measurements of molecular beam intensity as a function of background pressure (P_{B_∞}) and nozzle-skimmer distance. Their picture of the phenomena is that of background particles freely interpenetrating the jet flow up to some point. Closer to the orifice than this point, the background is quickly attenuated. Interpreted in this fashion, the molecular beam intensity measurements indicate an attenuation

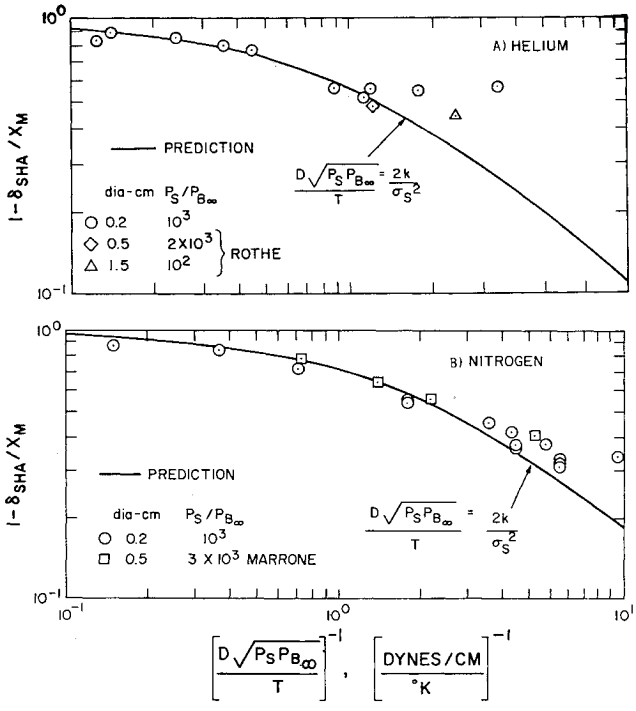

Fig. 5 Comparison of prediction from Eq. (5) and experiment: a) helium; b) nitrogen.

distance of about one-quarter of the distance between the orifice and the attainment of full background concentration on the jet axis. Fenn and Anderson[7] were able to correlate rather loosely their results as well as measurements from other workers by an empirical correlation scheme. Recent measurements have been made by Brown and Heald[8] under somewhat different conditions than all of the data which Fenn and Anderson used. The Brown and Heald data does not correlate very well with the earlier results.

Unfortunately, there is no existing theory that really indicates what parameters are important in this regime. An indication of the extent of the scattering regime is nonexistent. Even the nature of the regime or how perfect vacuum expansion or continuum flow may be approached from it has not been extensively discussed.

In order to obtain a physical and quantitative idea of what goes on in the scattering regime a simple analysis has been developed. The analysis is not rigorous; however, it does result in good quantitative comparisons with available data. It is useful for defining the limits and processes of the regime.

Thinking about the problem of how a very rarefied plume interacts with its environment produces several questions. Principally, there is some difficulty in forming a reasonable conceptual picture of how or what the scattering regime is and how it approaches its two limits of either perfect vacuum expansion or the beginning of continuum flow. One approach to the whole problem which seems to produce a good physical picture as well as quantitative results is to approximate the phenomena with a mathematically tractable physical model as follows.

Consider a small sonic orifice exhausting into a very large container. The walls of the container are such that they condense all jet particles that impinge on them. Allow test particles to evaporate from the condensate and proceed towards the source radially with a velocity $\bar{C}_B{}^1$ where $\bar{C}_B{}^1 = F\bar{C}_B$, F is some constant near unity, and $\bar{C}_B$ is the wall or "background" mean molecular speed where the temperature involved is that of the condensate surface.

The distance from the condensing surface to a point one mean free path of the test particle in the jet flow is λ, and the condensing surface is a distance l from the source as is illustrated by the schematic model in Fig. 6. It is easy to show that the distance $(l - \lambda)$, the "penetration distance" of a background molecule, is given by

$$\int_{l-\lambda}^{l} \frac{\pi \bar{V}_\infty \sigma_{Bj}{}^2 n^* r^{*2}}{\bar{C}_B{}^1 r^2}\, dr = 1 \tag{8}$$

For finite l,

$$l - \lambda = r_p - (r_p{}^2/l) + (r_p{}^3/l^2) \tag{9}$$

where

$$r_p = l - \lambda = \pi \bar{V}_\infty \sigma_{Bj}{}^2 n^* r^{*2}/\bar{C}_B{}^1$$

Thus when $l \gg r_p$, $(l - \lambda)$ approaches r_p and the penetration distance is dependent only on the source condition.

Rather than a single test particle, consider the situation in which a number of particles evaporate from the condensate; i.e., the back pressure has effectively been increased. Obviously, as long as these particles do not have a large number of self-collisions and as long as they move radially they will be attenuated or scattered as they move toward the source with an e folding distance of $r_p (l \gg r_p)$. There is of course a further complication when considering a random selection of background molecules. The general background particles does not move radially as the hypothetical test particle does, but can come from any place on the evaporating surface. It is assumed that background self-collisions are negligible as these molecules advance toward the source. One would generally expect, in the absence of scattering collisions,

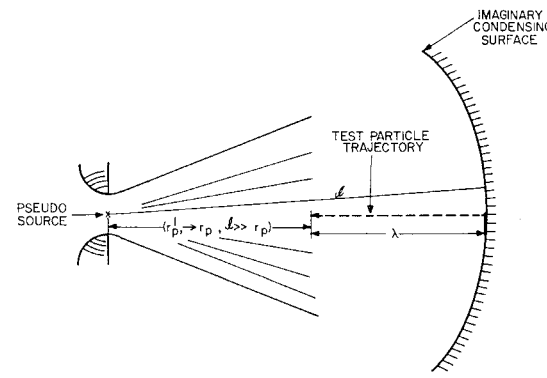

Fig. 6 Condensing surface model of a plume-background interaction.

molecules with motion in all directions. Moreover, the density would be uniform in space. However when there are collisions with oncoming jet molecules there will be an attenuation and velocity selection. To model this situation an equation that describes the density along a ray to the source is adopted. In the absence of scattering this equation states that the density is uniform. The effect of collisions is to produce an attenuation. The equation is

$$\bar{C}_B{}^1(dn_B/dr) = -\nu_{Bj} n_B \tag{10}$$

where the forcing of background into the jet must be related to the background thermal motion as represented by $\bar{C}_B{}^1$. If the background flow is written in spherical coordinates with a constant $\bar{C}_B{}^1$, the solution for n_B depends very sensitively on the arbitrary choice of the radius of a surface at which n_B is known. This difficulty is avoided by using the one-dimensional form of the equation. For the time being, the effect of background-background collisions will also be neglected which is consistent with the assumption that $l \gg r_p$.

In Eq. (10) ν_{Bj} is the background-jet collision frequency,

$$\nu_{Bj} = \epsilon \bar{V}_\infty \pi \sigma_{Bj}{}^2 n_j \tag{11}$$

Here, ϵ is a parameter less than or equal to one. It accounts for any uncertainty about how many of the model collisions are required before an average background particle has effectively been turned around or stopped. It might also be considered as an adjustment to the collision cross section based on viscosity measurements which certainly may not apply in the particular case of interest here.

From Eqs. (10) and (11)

$$dn_B/dr = -\epsilon \bar{V}_\infty \pi \sigma_{Bj}{}^2 n_j n_B/\bar{C}_B{}^1 \tag{12}$$

Approximate n_j by $n_{jI} = n^* r^{*2}/r^2$ and integrate to obtain

$$n_B/B_\infty = e^{-(r_p/r)} \tag{13}$$

where

$$r_p = \epsilon \bar{V}_\infty \pi \sigma_{Bj}{}^2 n^* r^{*2}/\bar{C}_B{}^1 \tag{14}$$

and r_p is the same as before except for the ϵ.

In calculating n_B, it has been assumed that n_j has not been affected by the background, an assumption which is reasonable under certain circumstances that will be discussed later.

Next the jet molecules are considered and assumed to be scattered by the background. In this case, a radial flow equation is necessary to describe the jet flow so that

$$(V_\infty/r^2)(dn_j r^2/dr) = -\nu_{jB} n_j \tag{15}$$

$$\nu_{jB} = \bar{V}_\infty \pi \sigma_{jB}{}^2 n_B \tag{16}$$

and Eq. (15) becomes

$$\ln\left\{\frac{V_\infty n_j r^2}{V_\infty n^* r^{*2}}\right\} = \frac{-\bar{V}_\infty \pi \sigma_{jB}{}^2 n_{B_\infty}}{V_\infty} \int_{r^*}^{r} e^{-r_p/r} dr \tag{17}$$

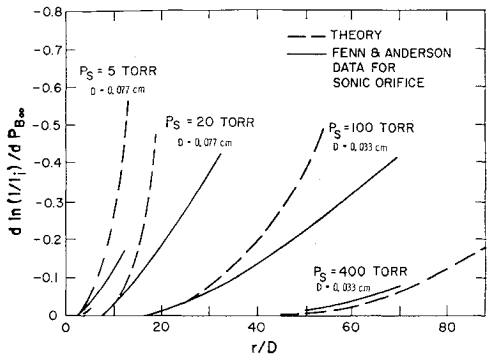

Fig. 7 Comparison of prediction from Eq. (24) and experiment.[7]

For $r_p \gg r^*$

$$\ln\left\{\frac{V_\infty n_j r^2}{V_\infty n^* r^{*2}}\right\} = \frac{\bar{V}_\infty \pi \sigma_{jB}{}^2 n_{B_\infty} r_p}{V_\infty} \int_\infty^{r_p/r} \frac{e^{-\eta}}{\eta^2}\, d\eta \qquad (18)$$

The interaction between jet and background has been set up this way because the experimental results of Fenn and Anderson[7] are sensitive to very small-angle scattering of the jet. Thus, significant molecular beam intensity decay due to scattering can be detected without the jet velocity and density field available for scattering background particles being significantly affected. Accordingly, the background-jet interaction has been decoupled by having the background scattered by an undisturbed jet but the jet scattered by a disturbed background. In the experiments $\sigma_{jB} \gg \sigma_{Bj}$ because the detection is sensitive to small-angle scattering of the jet particles. Another decoupling possibility will be seen later when $\sigma_{jB} = \sigma_{Bj}$, but both the jet and background scatter from essentially undisturbed scatterer density fields.

Equation (18) will now be put in a form suitable for comparison with Fenn and Anderson's data. Note that $\ln(V_\infty n_j r^2/V_\infty n^* r^{*2}) = \ln(I/I_i)$ where I is the molecular beam intensity that is predicted as a result of scattering by the background and I_i is the ideal flux $V_\infty n^* r^{*2}/r^2$. The primary data of Fenn and Anderson to which the predictions can be compared are presented in terms of $d\ \ln(I/I_i)/dP_{B_\infty}$. The Eq. (18) can be put in this form to give

$$\frac{d\ \ln I/I_i}{dP_{B_\infty}} = \frac{-\bar{V}_\infty{}^2 \epsilon \pi^2 \sigma_{jB}{}^2 \sigma_{Bj}{}^2 n^* r^{*2}}{V_\infty \bar{C}_B{}^1 k T_{B_\infty}} \left[\frac{r}{r_p}\, e^{-r_p/r} + E_i(-r_p/r)\right] \qquad (19)$$

where

$$E_i(-r_p/r) = \int_{r_p/r}^\infty \frac{e^{-\eta}}{\eta}\, d\eta \qquad (20)$$

and is tabulated by Jahnke and Emde.[9]

One feature of the physical situation that has not been taken into account is that the background particle may not come from infinity. Background-background collisions must dominate at some radius r_{crit} away from the source since n_j varies as $1/r^2$. It seems clear that a point where background-background collisions dominate can be approximated by the condensing surface of the present model being moved such that $l = r_{crit}$. The critical surface radius can be chosen in numerous ways, all of which turn out to be essentially equivalent. One physically realistic choice is the distance r at which the background-background collision frequency equals the background-jet collision frequency or $\nu_{Bj} = \nu_{BB}$. From this condition

$$r_{crit}{}^2 = \frac{\bar{V}_\infty \pi \sigma_{Bj}{}^2 0.161 n_s D^2}{\bar{C}_B{}^1 \pi \sigma_{BB}{}^2 n_{B_\infty}} \qquad (21)$$

If the radius r_{crit} is used to supply the boundary condition for the background scattering equation, all that changes is the constant of integration and

$$n_B = n_{B_\infty} e^{-(r_p/r_{crit})[(r_{crit}/r)-1]} \qquad (22)$$

where the point at which $n_B = n_{B_\infty}/e$ will be called $r_p{}^1$.

From Eqs. (14) and (22) the ratio

$$\frac{r_p}{r_{crit}} = \pi \epsilon (0.161)^{1/2} D (n_s n_{B_\infty})^{1/2} \sigma_{Bj} \sigma_{BB} (\bar{V}_\infty/\bar{C}_B{}^1)^{1/2} \qquad (23)$$

If $r_p \ll r_{crit}$ Eq. (22) reduces to Eq. (13). As $r_{crit} \to r_p$ the background penetration distance $r_p{}^1$ becomes less as background is forced closer to the source. At large r_{crit} the background penetration is independent of the background concentration. However, if $r_{crit} \to r_p$ the penetration distance $r_p{}^1$ becomes a function of background concentration through the term $e^{r_p/r_{crit}}$. This was of course expected from the earlier mean free path calculation of Eq. (9).

From Eq. (15) and (22)

$$\frac{d\ \ln I/I_i}{dP_{B_\infty}} = \frac{-\bar{V}_\infty \pi \sigma_{jB}{}^2 r_p e^{r_p/r_{crit}}}{V_\infty k T} \left\{\frac{r}{r_p}\, e^{-r_p/r} + E_i\left(\frac{-r_p}{r}\right)\right\} \qquad (24)$$

The results of this analysis were compared to the data of Fenn and Anderson.[7] In order to do so, several adjustable parameters are available in the analysis. While the choice of these is arbitrary within limits they must be kept the same for all of the experimental results. The parameters were chosen as follows. The relative velocity factor $F = 1$, the parameter $\epsilon = 0.5$, the small-angle scattering cross section for the jet particles 1.49×10^{-14} cm^2; the other cross sections were based on the normal viscosity cross section for argon. Temperature, pressure, and dimensions were chosen to correspond to the experimental conditions.

Comparison of the predictions and experiments are shown in Fig. 7. For small amounts of scattering, the theory predicts the observations. For large amounts of scattering the theory and the results separate. Part of the mismatch may lie in the indirectness of the molecular beam intensity measurement as an indication of the presence of background. No attempt was made in the theory to account for the complicated sampling process involved or to account for scattered molecules which may have been measured in the experiment.

The comparison of the experiment and theory is particularly interesting for the 400 torr case (Fig. 7). For this condition the term $e^{r_p/r_{crit}}$ is not small. As can be seen, the r_{crit} correction seems to account satisfactorily for this effect. In all other cases the r_{crit} terms are not significant, and the penetration simply scales with the source condition as predicted by the theory.

In the calculation, the background does not build very rapidly to its undisturbed value, but takes several times r_p

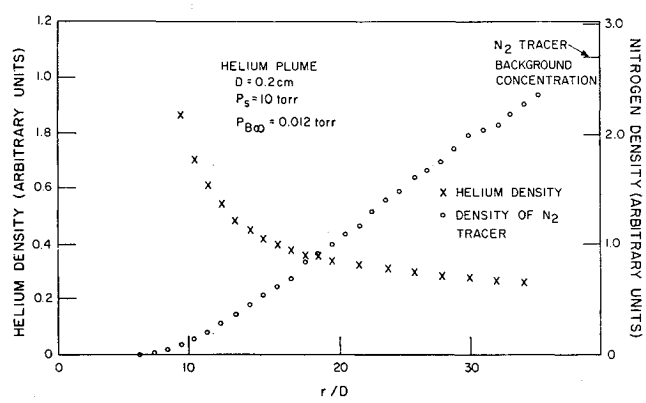

Fig. 8 Background penetration along plume centerline.

to do so. This picture is somewhat at odds with the rapid buildup of background to n_{B_∞} on the order of one-quarter r_p, interpreted by Fenn and Anderson from their molecular beam measurements. Some electron beam measurements of background density along the jet centerline that have been obtained very recently shows that the background does not build rapidly.

In these experiments, the helium plume from a 2 mm diam orifice was examined. The background gas was helium from the jet flow, but a trace of nitrogen was added to the background by means of a controlled leak into the test chamber at a position away from the plume. Both helium and nitrogen density were measured along the jet axis using the electron beam fluorescence technique (Ref. 3 and Sec. 2). The data in Fig. 8 shows the nitrogen background tracer slowly rises and has not reached the background level at the last measured point.

More experimental evidence is needed in order to construct a good picture of all the details of the background behavior; however, the analysis of the jet scattering presented here seems to have captured the important physical characteristics of the phenomena. The results of the analysis will now be used to indicate how the scattering region, as outlined, goes to the limits of pure vacuum expansion and to the low density limit of the transition regime.

Consider the form of the jet decay curve where interest lies not in small-angle scattering but in decay of the jet intensity as a result of collisions involving significant momentum transfer. In this case $\sigma_{jB} = \sigma_{Bj}$. The jet scattering curve, Eq. (17), becomes

$$\ln \frac{V_\infty n_j r^2}{V_\infty n^* r^{*2}} = \frac{-\bar{V}_\infty \pi}{V_\infty} \sigma_{jB}{}^2 n_{B_\infty} \int_{r^*}^{r} e^{-r_p/r} dr$$

if

$$r^* \ll r_p \ll r, \int_{r^*}^{r} e^{-r_p/r}\, dr \to \int_0^r dr \tag{25}$$

or

$$\ln \frac{V_\infty n_j r^2}{V_\infty n^* r^{*2}} = \frac{-\bar{V}_\infty}{V_\infty} \pi \sigma_{jB}{}^2 n_{B_\infty} r \tag{26}$$

which applies where the n_{B_∞} is sufficiently low to preclude significant jet scattering in a region where n_B is being reduced by scattering.

The point where the jet flux has dropped to $1/e$ of its ideal value is noted by $r_{1/e}$ or from Eq. (26)

$$r_{1/e} = \frac{V_\infty}{\bar{V}_\infty \pi \sigma_{jB}{}^2 n_{B_\infty}} \tag{27}$$

As long as $r_{1/e} \gg r_p$, the two scattering zones, one for the background by the jet and the other for the jet by the background are separable. The decoupled scattering zones can be represented as shown in Fig. 9. The background penetration is governed by the source condition, the jet scattering zone by background conditions. The perfect vacuum limit is approached by lowering n_{B_∞} since $r_{1/e}$ varies inversely as n_{B_∞}. Either increasing n_{B_∞} or increasing the source density will tend to reduce the scattering zone thickness $(r_{1/e} - r_p)$. When this thickness becomes somewhat less than its average value, the formation of a thick shock continuum-like flow has begun. The flow is transferring from the scattering to the transition regime. Based on the decoupled expressions for $r_{1/e}$ and r_p, it is suggested that the plume is at the boundary between the scattering and transition regimes when $r_p = r_{1/e}$.

Applying this condition and remembering $\sigma_{jB}{}^2 = \sigma_{Bj}{}^2 = \sigma_M{}^2$

$$D^2 n_{B_\infty} n_s = \frac{V_\infty \bar{C}_B{}^1}{0.161 \epsilon \pi \bar{V}_\infty{}^2 \sigma_M{}^4} \tag{28}$$

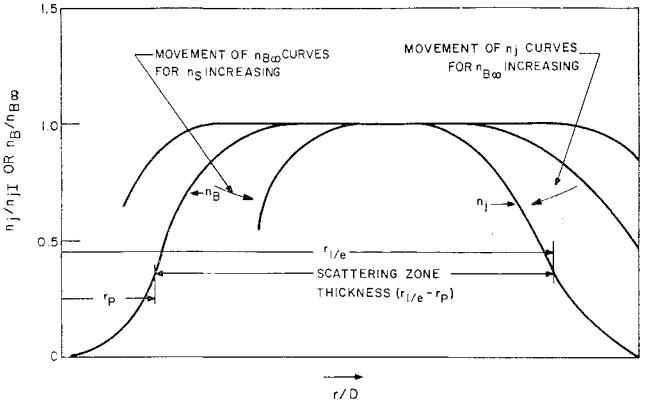

Fig. 9 Representation of the scattering zone of a plume's interaction with background gas in the most rarefied portion of the scattering regime.

For equal stagnation and background temperatures Eq. (28) can be put in the form

$$\frac{D(P_s P_{B_\infty})^{1/2}}{T} = \frac{k}{\sigma_M{}^2} \left\{ \left(\frac{V_\infty \bar{C}_B{}^1}{0.161\epsilon} \right)^{1/2} \Big/ \pi \bar{V}_\infty \right\} \tag{29}$$

For $\epsilon = 0.5$, $\bar{C}_B{}^1 = \bar{C}_B$ $(F = 1)$ the quantities in the bracket on the right hand side of Eq. (29) reduce to a value of around 0.6. Thus the boundary between transition and scattering occurs for values of ξ in the range

$$\frac{0.6k}{\sigma_s{}^2} \leq \xi = \frac{D(P_s P_{B_\infty})^{1/2}}{T} \leq \frac{2k}{\sigma_s{}^2} \tag{30}$$

For $\xi < 0.6k/\sigma_M{}^2$ the scattering regime is applicable for $\xi > 2k/\sigma_M{}^2$ the transition regime of thick shock waves applies. Note that the scattering analysis produces the same grouping of independent variables as was obtained from the analysis of the transition regime.

The radius at which the scattering zone collapses to something resembling a shock wave is of interest; it should have the same characteristics as the shock envelope of the continuum plume.

For $r_{1/e} = r_p = r_{X_M}$, two equivalent relations can be written from Eqs. (14) and (27) and manipulated to obtain for helium

$$\frac{r_{X_M}}{D} = \left(\frac{0.161 \epsilon V_\infty}{\bar{C}_B{}^1} \right)^{1/2} \left(\frac{P_s}{P_{B_\infty}} \right)^{1/2} \tag{31}$$

$$\frac{r_{X_M}}{D} \approx 0.4 \left(\frac{P_s}{P_{B_\infty}} \right)^{1/2} \tag{32}$$

Compare the relationship in Eq. (32) to the behavior of the Riemann wave in a continuum plume as given by Eq. (1).

The decoupling of the two scattering zones must occur when say $r_{1/e} \geq 10 r_p$ which gives by suitably altering Eqs. (28) and (29)

$$\frac{D(P_s P_{B_\infty})^{1/2}}{T} \leq \frac{0.2k}{\sigma_M{}^2} \tag{33}$$

It is well to remember that with this analysis there are constraints on the $P_s D$ product in order to ensure a continuum expansion near the throat. Thus very low values of ξ must be obtained by reducing n_{B_∞}. It is in this manner that the perfect vacuum expansion can be attained.

Finally, if the penetration distance r_p is divided by the characteristic distance X_M, it is found that

$$\frac{r_p{}^1}{X_M} = f \left(\frac{D(P_s P_{B_\infty})^{1/2}}{T} \right) \tag{34}$$

Thus, the rarefaction in the scattering regime as indicated by $r_p{}^1$ (or r_p) scales with the same rarefaction parameter as the shock broadening in the transition regime. Evidently the parameter $D(P_sP_{B_\infty})^{1/2}/T$ can be used to scale certain aspects of plume rarefaction for a wide range of conditions.

4. Conclusions

The transition from continuum flow to perfect vacuum expansion of the plume from an underexpanded sonic orifice has been described. Certain features of the entire rarefaction process can be scaled with the rarefaction parameter $D(P_sP_{B_\infty})^{1/2}/T$ that has been derived in this paper. The broadening of the shock waves bounding the plume, the penetration of background gas into the plume and the eventual transition to perfect vacuum expansion have all been considered.

References

[1] *Rarefied Gas Dynamics*, National Committee on Fluid Dynamics Films.

[2] Maguire, B. L., Muntz, E. P., and Mallin, J. R., "Visualization Techniques for Low-Density Flow Fields," *IEEE Transactions on Aerospace and Electronic Systems*, Vol. AES-3, No. 2, March 1967, pp. 321–326.

[3] Muntz, E. P. and Marsden, D. J., "Electron Excitation Applied to the Experimental Investigation of Rarefied Gas Flows," *Rarefied Gas Dynamics, Third Symposium*, Vol. II, Academic Press, New York, 1963, pp. 495–526.

[4] Schumacher, B. W. and Gadamer, E. O., "Electron Beam Fluorescence Probe for Measuring the Local Gas Density in a Wide Field of Observation," *Canadian Journal of Physics*, Vol. 36, 1958, p. 654.

[5] Ashkenas, H. and Sherman, F. S., "The Structure and Utilization of Supersonic Free Jets in Low Density Wind Tunnels," *Rarefied Gas Dynamics, Fourth Symposium*, Vol. II, Academic Press, New York, 1966, pp. 84–105.

[6] Talbot, L. and Sherman, F. S., "Structure of Weak Shock Waves in a Monatomic Gas," Rept. HE-150-137, May 1956, Univ. of California.

[7] Fenn, J. B. and Anderson, J. B., "Background and Sampling Effects in Free Jet Studies by Molecular Beam Measurements," *Rarefied Gas Dynamics, Fourth Symposium*, Vol. II, Academic Press, New York, 1966, pp. 311–330.

[8] Brown, R. F. and Heald, J. H., "Background Gas Scattering and Skimmer Interaction Studies Using a Cryogenically Pumped Molecular Beam Generator," *Rarefied Gas Dynamics, Fifth Symposium*, Vol. II, Academic Press, New York, 1967, pp. 1407–1424.

[9] Jahnke, E. and Emde, F., *Tables of Functions*, Dover, New York, 1945.

[10] Rothe, D. E., "Electron Beam Studies of the Diffusive Separation of Helium-Argon Mixtures," *The Physics of Fluids*, Vol. 9, No. 9, Sept. 1966, pp. 1643–1658.

[11] Marrone, P. V., "Rotational Temperature and Density Measurements in Underexpanded Jets and Shock Waves Using an Electron Beam Probe," Rept. 113, 1966, Univ. of Toronto, Inst. for Aerospace Studies.

SEPTEMBER 1970 AIAA JOURNAL VOL. 8, NO. 9

Drag Coefficients for Free Molecule Flow in the Velocity Range 7–37 km/sec

J. W. Boring* and R. R. Humphris†
University of Virginia, Charlottesville, Va.

Measurements have been made of the momentum transfer by a beam of N_2 molecules to solid surfaces for molecular energies of 8–200 ev (velocity range 7–37 km/sec). The results of these measurements allow one to calculate drag coefficients for the situation where nearly monoenergetic molecules all moving in the same direction impinge upon a solid convex body. Drag coefficients for N_2 molecules striking spheres of Echo I and Echo II satellite material are found to be in the range 1.9–2.2.

Introduction

SINCE the advent of Earth satellites there has been intense interest in particle-surface interactions for relative velocities in the range 7–11 km/sec. However, there is only a small amount of experimental information available concerning these interactions for neutral species because of the inherently awkward techniques that must be employed in order to achieve velocities in this range. In using satellites to gain information concerning the density of the earth's upper atmosphere, one is particularly interested in the drag produced on the satellite by the atmosphere and hence in the manner in which atoms and molecules exchange momentum with the surfaces of the satellite. The present paper describes laboratory measurements of the momentum transfer to solid surfaces by N_2 molecules in the energy range 8–200 ev (velocity range 7–37 km/sec). The results are obtained as a function of the angle of incidence, thereby permitting one to calculate drag coefficients for solid bodies of arbitrary convex shape moving through a gas that has thermal motion that is negligible compared to the velocity of the body.

Consider now the drag on a satellite moving through a rarefied atmosphere (free molecular flow) with a speed large, compared to the thermal motion of the atmospheric molecules. The drag coefficient can then be expressed as

$$C_D = \frac{F}{\frac{1}{2}A\rho v_0^2} = 2\left[1 + \frac{1}{A}\int_s \frac{P_m}{P_0}\cos\theta da\right] \quad (1)$$

Received March 24, 1969; revision received March 30, 1970. This research was supported by NASA under Contract NAS1-2538.

* Associate Professor, Department of Aerospace Engineering and Engineering Physics.

† Senior Scientist, Research Laboratories for the Engineering Sciences.